

# UAV-SfM topographic stream survey:

Modelling underwater topography using  
UAV-based structure from motion  
photogrammetry

October

2021

Yingjie Ye

Dissertation for BE(Hons), Forest Engineering

Supervised by Professor Rien Visser

Supported by Hancock Forest Management (NZ)



## **Acknowledgement**

I would like to express my special thanks to my Mum and Dad for all the support and trust throughout the journey of my life. I would like to thank Rien Visser and Campbell Harvey for coaching and assisting me through the project. I would also like to acknowledge Hancock Forest Management and WIDE Trust for the support of this project. Special thanks also go to Cameron Jin, Perry Han, Hang Wang for helping me to collect the data in the cold water. I would like to thank my girlfriend Eugenia for the love and support. Finally, I would like to thank all the people I met in Aotearoa, New Zealand, you made me feel like home here.

## Executive Summary

This report aims to find an UAV (Unmanned Aerial Vehicle) based photogrammetry topographic stream survey workflow that can achieve a level of accuracy that suits the forestry stream crossing design purpose. The experiment data was captured in a stream in Halswell, Christchurch ((43°35'15.3" S, 172°33'19.3" E), including three sets of aerial imagery and one set of terrestrial survey data. The imagery was post-processed into nine models with three workflow variations. The accuracy of the models was validated by the terrestrial survey data. The findings of the study may be of interest to forest engineers and/or harvest planners who want to use UAVs to assist stream crossing design.

The imagery was captured by UAV from 30 m and 50 m altitude above ground level with and without the use of ground control points (GCPs). The imagery was post-processed using photogrammetry structure-from-motion (SfM) software (Agisoft Metashape Pro) into dense point clouds, which are collection of points that represent 3D terrain or objects in real world.

The main challenge of using UAV photogrammetry to survey underwater topography is that the refraction of light into water will cause underestimation of water depth and thus the stream bed elevation. To address this issue, the models are corrected by small-angle and multi-angle correction methods. These two workflows manipulate the point clouds according to the camera angle and water depth. The multi-angle correction method together with the images captured 30 m above ground level and GCPs achieved the best accuracy with a mean error of -0.011 m and a root-mean-square error (RMSE) of 0.145 m. By using this method, the mean error is reduced by 0.081 m and the RMSE is reduced by 0.032 m from the uncorrected model. Although the multi-angle method can achieve the best accuracy, for the small site with relatively simple terrain used in this study, the improvement of accuracy over the small-angle method is not obvious (ca. 0.01 m in mean error and no improvement in RMSE).

To test the consistency of the proposed workflow, a second study was performed at another stream in Christchurch with deeper streambed and slightly higher flow rate. The results show consistency with the first study, with a mean error of 0.022 m, an error standard deviation of 0.105, and RMSE of 0.105 m.

From this study, the use of GCPs is recommended since it can ensure the quality of SfM processing and georeferencing accuracy of the model. The refraction correction is essential for achieving satisfactory survey accuracy for the submerged area. For sites with simple terrain, the small-angle correction method can achieve almost the same level of accuracy with a simpler workflow, when compared to multi-angle correction method. Since the study area is relatively simple, future studies can be conducted at places with more complex terrain and canopy cover conditions to check if multi-angle correction method can achieve a more promising result. In addition, the multi-angle correction method can be automated and integrated as a tool into photogrammetry or GIS software packages.

# Table of Contents

Acknowledgement .....	2
Executive Summary.....	3
Background .....	6
1. Introduction .....	7
2. Literature review.....	8
2.1 The necessity of stream survey.....	8
2.2 Accuracy required for stream crossing design.....	10
2.3 Workflow.....	13
2.4 Improve accuracy .....	16
3. Materials and Methods.....	18
3.1 Study area description .....	18
3.2 Ground control points set-up and validation data collection.....	19
3.3 Photogrammetry data acquisition .....	19
3.4 Structure from Motion processing .....	20
3.5 Refraction correction .....	21
3.6 Validation of data.....	23
3.7 Test the proposed workflow in another site .....	24
4. Results.....	25
4.1 SfM quality .....	25
4.2 Error statistics .....	25
4.3 Ground control points.....	27
4.4 Flight height .....	27

4.5 Error versus water depth .....	28
4.6 Performance of refraction correction.....	28
4.7 Results from the second study .....	29
5. Discussion.....	30
5.1 Relative accuracy versus absolute accuracy .....	30
5.2 Efficacy of the different workflows.....	31
6. Conclusion.....	33
7. References .....	34

## Background

The construction of forestry roads usually involves crossing rivers. In New Zealand, it is enforced by laws and regulations such as; The National Environmental Standards for Plantation Forestry (NES-PF), the Freshwater Fisheries Regulations 1983 (FFR83), regional plans and district plans that crossing structures must meet certain serviceability, environmental, and safety requirements. All these requirements need to be accommodated in the stream crossing design. The stream crossing design requires good knowledge of the stream topography, and the accuracy of topographical stream survey will affect the quality of overall design. Therefore, achieving a satisfactory survey accuracy is essential for a good stream crossing design.

UAV-based Structure-from-Motion photogrammetry (SfM) is a low budget and user-friendly remote sensing technology used by many New Zealand forestry companies. The common forestry applications include forest inventory, quarry stock management, cutover mapping, windthrow assessment etc. Recent studies in the UAV remote sensing field show that UAV photogrammetry technology has the potential to perform accurate survey of stream topographies, including the exposed and submerged bed substrate. However, there are no studies demonstrating that UAV photogrammetry can be used for the purpose of forestry stream crossing design.

This idea of this project originated from the UAV survey and culvert design experience during my 2020 summer internship. The efficiency that the drone technology demonstrated for surveying the quarry stockpile was amazing. This made me curious about the possibility of using drones to survey stream channels to achieve a similar level of accuracy as the dry area.

# 1. Introduction

Structure from Motion photogrammetry (SfM) is an emerging technology for acquiring 3D spatial data in forestry. The adoption of SfM allows users to produce high accuracy survey results at little cost with minimal training (Iglhaut et al., 2019). According to a survey on 29 New Zealand forest companies that manage over 80% of New Zealand's plantation forest estate; 83% of companies use Unpiloted Aerial Vehicles (UAVs) as a platform to collect aerial imagery (De Gouw et al., 2020). The most common workflow is UAV-SfM photogrammetry, which is the survey technique that uses UAVs to capture a sequence of images in grid patterns, then stitch the images together to produce a dense point cloud that represents real-world terrains and above-terrain structures (e.g. trees). SfM allows users to perform ascertain measurements of objects. This survey technique is widely used in forestry sector. Examples of forestry applications include forest inventory (Piermattei et al., 2019), cutover mapping, windthrow damage assessment, post-harvest waste assessment (Riedinger, 2020), quarry management (Rossi et al., 2017) and monitoring road impacts on waterways (Brown & Visser, 2018), etc.

As with other survey techniques, the accuracy of UAV-SfM survey depends on how the surveyor performs the survey and the environmental factors of the site. There are many factors that affect the accuracy of UAV-SfM, which include:

- survey quality: flight parameters, devices attributes, presence of ground control points (GCPs) or on-board RTK/PPK, data processing quality, etc.
- environmental conditions: clouds, shadows, glares, etc.
- survey area complexity: topographic complexity, presence of vegetation and water, etc.

A properly set up UAV mapping plan in favourable environmental conditions can output satisfactory results. Recent studies show that UAV-SfM can generate outputs with high levels of detail and accuracy for general road design purposes such as measuring slopes, calculating earthwork volumes, accessing slope stability, etc (Akgul et al., 2018; Zulkipli & Tahar, 2018).

Stream crossing design is an integral part of road design as road access to forested areas often need to cross streams. Knowledge of site topography and channel geometry are necessary for a successful stream crossing design. When a UAV-SfM survey technique is used for mapping submerged area without proper adjustment or correction, the accuracy of submerged area can be significantly lower than exposed area due to the refraction effect and disturbance of water. Other remote sensing methods such as multi-beam echo sounder, satellite imagery or LiDAR often require specialised equipment and survey techniques, extensive in-channel calibration data, interpolation between points or are simply unavailable. Therefore, when it comes to mapping submerged areas, traditional topographic survey methods are still commonly used. Such methods are time consuming, labour intensive and sometimes difficult to access to survey areas. Also, traditional survey requires interpolation between coarse point data, which makes the output less detailed. A number of solutions for improving mapping accuracy for submerged areas have been proposed. These solutions will be introduced in the literature review section.

The aim of this study is to explore a feasible method that can generate outputs with the level of accuracy that meet the requirement of stream crossing design purposes. Also, to test if it is possible to achieve the desired level of accuracy without the use of ground control points by trialling several refraction correction techniques. The data processing complexity and expertise required will also be explored. The complete workflow, especially the data processing techniques will be recorded, which will be helpful for forest engineers or project planners who want to use these survey techniques to assist their stream crossing designs.

## **2. Literature review**

### ***2.1 The necessity of stream survey***

Roads access to forested areas often need to cross streams. When designing stream crossing structures, it is required by New Zealand legislation to provide proper fish passage. In New Zealand, there are approximate 35 native fish species. Over half migrate up river as juveniles (Forest Growers Levy et al., 2020). Section 40 of the National Environmental Standards for Plantation Forestry (NES-PF) stipulates that for permitted activities, river crossings must provide fish passage upstream and downstream and maintain river bed material. These are the minimum requirements that need to be met when designing stream crossings.

In order to prompt better management of fish passage requirements, a guideline for New Zealand fish passage has been introduced (Franklin et al., 2018). According to the guideline, due to the structural features, bridges, temporary bridges and large open bottom culverts provide better fish passage than other types of structures, so they can be designed without specific consideration of fish passage. Ford crossings are least favourable option for fish passage. In comparison, the fish passage capability of culvert structures including single culvert, box culvert and battery culverts are mostly affected by the design.

#### **2.1.1 Hydraulic design**

There are two types of culvert design depending on the purpose of the design. One is called hydraulic design, which is to design the culvert to meet the hydraulic conveyance requirement while minimising the size. While this is not mutually exclusive with the objective of providing fish passage, there is certain contradiction between the two purposes. In the context of hydraulic design, the idea of ensuring fish passage is to limit the high flow water velocity and low flow water depth in the culvert. For water velocity, if there is no specific reference for fish swimming ability, a simpler approach is to ensure that the water velocity in culvert is consistent with that of the adjacent river section. To calculate the water velocity, two inputs are required, one is the base flow. 20% exceedance flow is used as the high base flow. NZ River Maps by NIWA (the National Institute of Water and Atmospheric Research) is a useful tool to access modelled base flows.

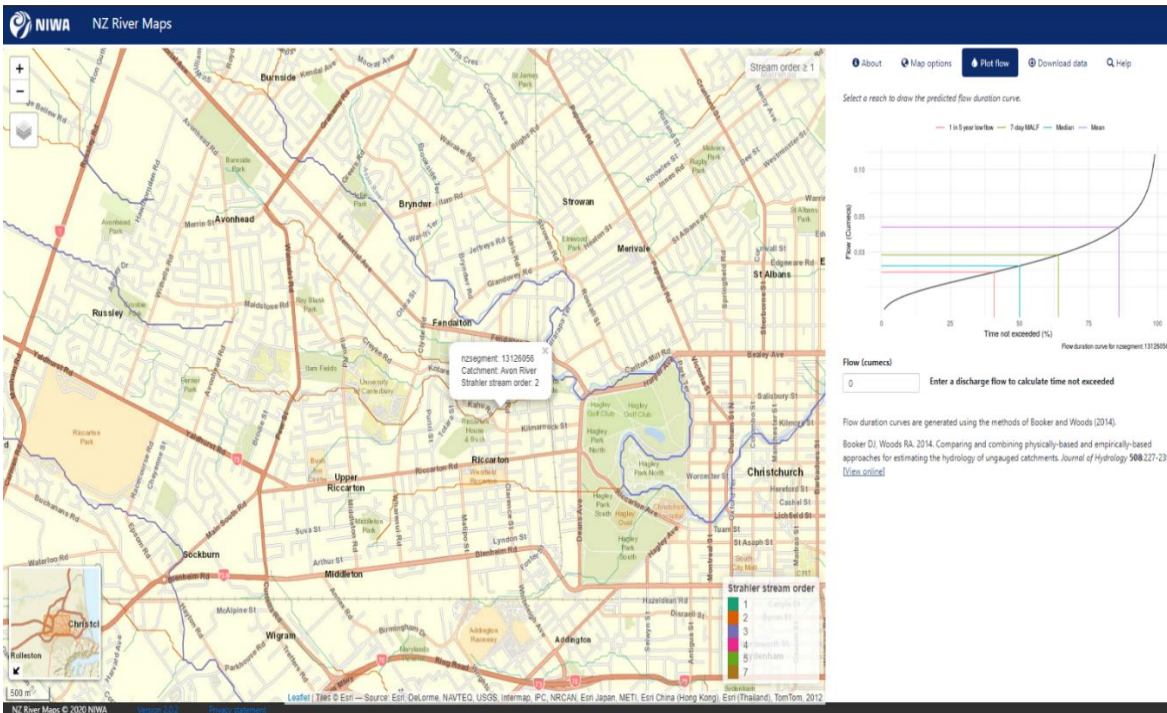


Figure 1. NZ River Maps by NIWA

The flow duration curve on the screenshot above allows the user to find 20% exceedance flow. Another input required is the wetted cross-sectional area of the adjacent river section. The figure below shows the definition of wetted cross-sectional area.

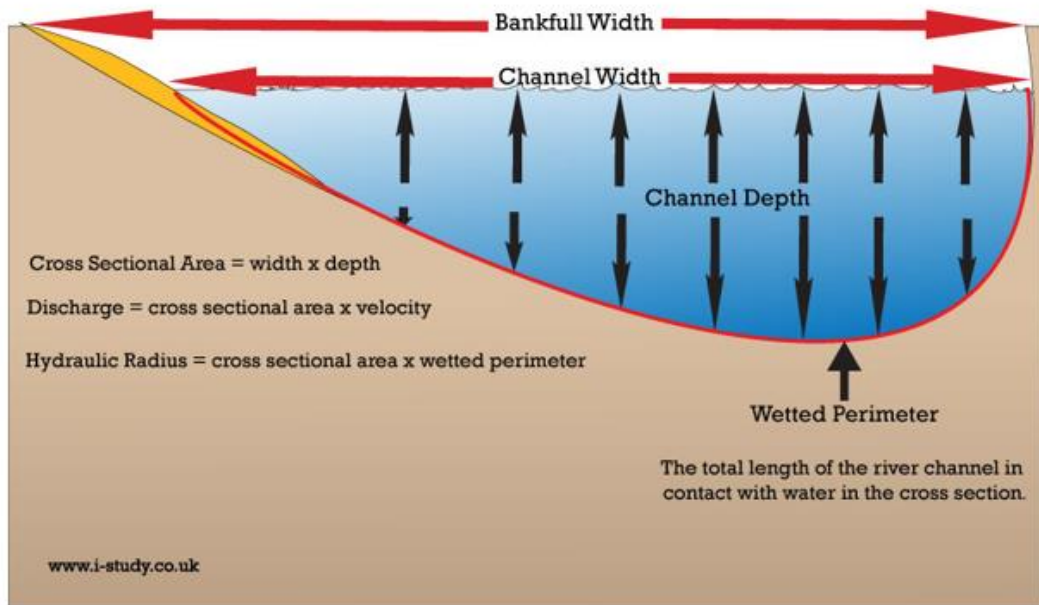


Figure 2. Cross-sectional view of the stream

Note. From “New Zealand Fish Passage Guidelines”, by P. Franklin, et al., April, 2018, NIWA (<https://niwa.co.nz/sites/niwa.co.nz/files/NZ-FishPassageGuidelines-upto4m-NIWA-DOC-NZFPAG.pdf>). Copyright 2021 by NIWA.

The water velocity is flow rate divided by wetted cross-sectional area. The average water velocity then can be used as the allowable water velocity. The cross-sectional area can be directly measured from the 3D model generated by UAV-SfM survey. It is worth noting that because the velocity is based on a theoretical flow rate, the velocity from direct measurement (e.g., stream gauging or ‘orange peel’ method) is the velocity at a certain point and is not the allowable water velocity. Another design parameter, which is the minimum water depth, also needs the channel geometry as an input. More detail can be found in page 52 – 53 of NZ Fish Passage Guidelines (Franklin et al., 2018).

### **2.1.2 Stream simulation design**

In the guideline, the hydraulic design method is described as the minimum design standard. The best practice of culvert fish passage design method is stream simulation. This method retains or restores the natural stream bed after construction and provides the heterogeneity in water depth and flow velocity. The required level of detail of site assessment is higher than hydraulic design. It is specified in the site assessment section that a geomorphic information and topographic survey of the reference section are the necessary elements of the site assessment. The guideline suggests detailed site assessment procedures should be referred to Chapter 5 of U.S. Department of Agriculture (United States. Forest Service. Stream-Simulation Working Group. & Technology & Development Program (U.S.), 2008).

Except from the requirements of fish passage design, a high-resolution topographic map of the site allows the planner to prepare site plan, construction contract and environmental management plans (e.g. monitor sediment and erosion before and after harvest operation). In addition, it also allows the planner to check site characteristics such as bed invert gradient to determine if the stream crossing construction would require a resource consent under NES-PF.

### ***2.2 Accuracy required for stream crossing design***

Accuracy refers to the closeness of the measurement result to the standard or actual values. To understand the level of accuracy required for stream crossing design, two questions need to be answered. One is how to measure and report accuracy. The other is how accurate the results need to be in order to fulfil the design purpose.

Land Information New Zealand (LINZ) has a specification regards to measuring and reporting geospatial accuracy (LINZ, 2009a). In this standard, vertical accuracy is expressed as:

$$VE_{95} = 1.96\sigma_z$$

where  $VE_{95}$  is the vertical accuracy at 95% confident level,  $\sigma_z$  is the standard deviation of error in vertical coordinate.

And the horizontal accuracy is the radial or two-dimensional accuracy of X & Y direction.

$$HE_{95} = \frac{2.45}{\sqrt{2}} \sqrt{\sigma_x^2 + \sigma_y^2}$$

where  $\sigma_x$  is the standard deviation of error in x coordinate and  $\sigma_y$  is the standard deviation of error in y coordinate.

This method may lead to a bias as shown in Figure 3 below:

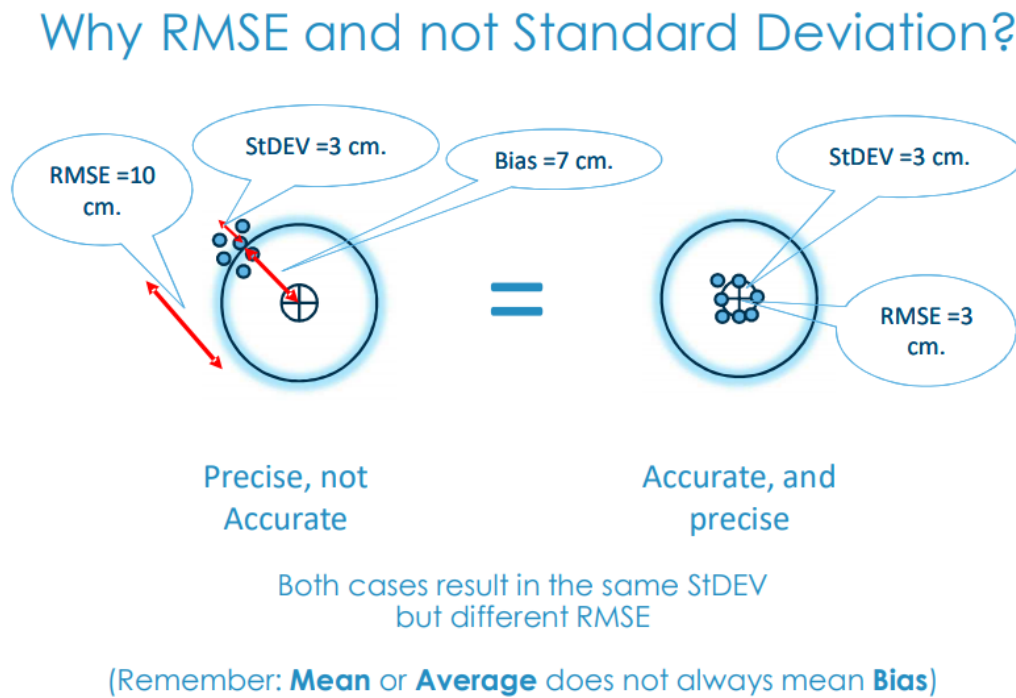


Figure 3. RMSE vs Standard deviation in describing accuracy

where cases with same standard deviation may have different level of accuracy. To reflect the accuracy properly, American Society for Photogrammetry and Remote Sensing (ASPRS) adopted a new standard (ASPRS, 2014), which use root-mean-square error (RMSE) to address the accuracy. The equation for RMSE is:

$$RMSE = \sqrt{\frac{\sum(Z - Z_i)^2}{n}}$$

where  $Z$  is the measured value from the output survey map,  $Z_i$  is the control value (measured from a more accurate survey method),  $n$  is the number of measurements.

The equation of RMSE is very similar to standard deviation, but the term  $Z_i$  in standard deviation is replaced by mean value of error.

Different purposes of project design require site assessments with different levels of accuracy. There is no specific standard for the stream crossing structure in forestry sector. But standards of other design & construction projects with similar complexity can be referred to as a benchmark. The following table lists standards used by government authorities and societies in the U.S.A. and also a standard for NZTA state highway surveys.

Table 1. Requirements on accuracy for crossing design survey and general photogrammetry survey.

Name	Organisation	Purpose	Horizontal Accuracy	Vertical Accuracy	Reference
Geospatial Positioning Accuracy Standards for Architecture, Engineering, Construction and Facility Management	National Spatial Data Infrastructure	Grading and Excavation Plans (Roads, Drainage, Curb, Gutter etc. - Field construction layout)	0.25 m	0.1 m	(National Spatial Data Infrastructure, 2002)
Accuracy Standards for Digital Geospatial Data	American Society for Photogrammetry and Remote Sensing (ASPRS)	U.S. technical requirements of planimetric and vertical accuracy of photogrammetry surveys	0.1 m	0.1 m	(ASPRS, 2014)
Project Management and Design Manual	U.S. Department of Transportation	Building or structural design – Bridges, Structures, Culverts, Walls	0.13 m	0.2 m	(U.S. Department of Transportation, 2018)
State highway professional services contract proforma manual	Waka Kotahi NZ Transport Agency	Carriageways and solid surfaces, culvert inverts, drainage system water levels and inverts	0.05 m	0.05 m	(NZTA, 2021)

It is worth noting that the NZTA standard is for state highway projects, the level of accuracy is significantly higher than other standards for culverts or bridges. In practice, the required level of accuracy of survey often depends on the experience of the project designer or best available data.

## 2.3 Workflow

The workflow of UAV-SfM stream survey is similar to a regular UAV-SfM survey. The only difference is to identify the submerged area and apply a uniform or spatially-dependent correction to the submerged area. A UAV-SfM mapping workflow has the following steps:

### 2.3.1 Survey design

Survey design needs to determine the survey boundary, equipment, flight plan software, flight mission parameters, usage of ground control points (GCPs) according to the required accuracy and the complexity of the survey location. According to NZ Fish Passage Guidelines (Franklin et al., 2018) for stream simulation design, a reference reach should be covered in the survey area. Figure 4 shows the concept of a reference reach.

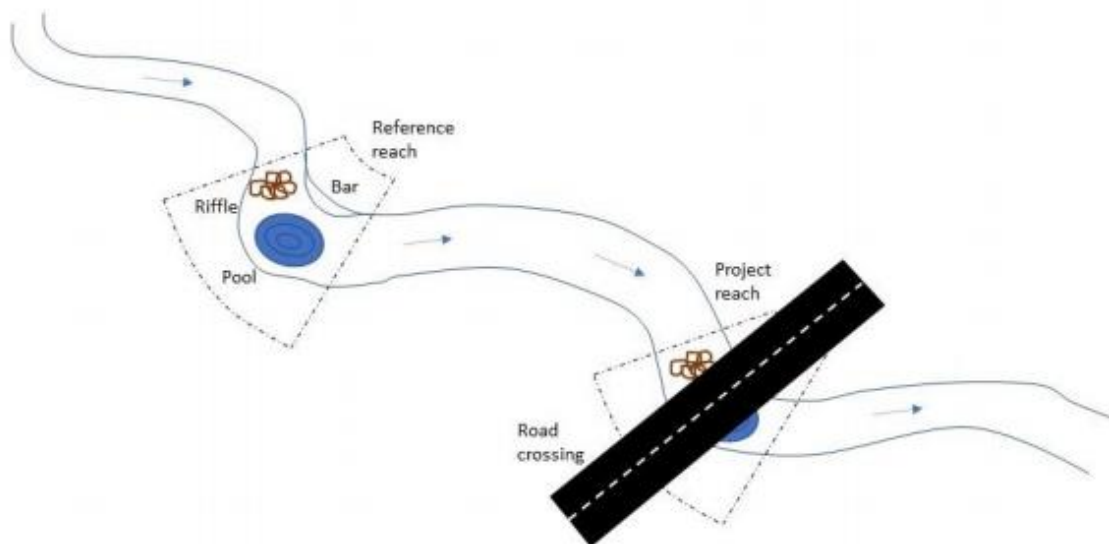


Figure 4. Reference reach for stream simulation design.

Note. From “New Zealand Fish Passage Guidelines”, by P. Franklin, et al., April, 2018, NIWA (<https://niwa.co.nz/sites/niwa.co.nz/files/NZ-FishPassageGuidelines-upto4m-NIWA-DOC-NZFPAG.pdf>). Copyright 2021 by NIWA.

For hydraulic design, the survey area should cover 20 – 30 channel widths in the longitudinal direction along the channel. As an example; for a river with a 5 meter bankfull width, the survey

area should cover 100 – 150 meters of channel length. This ensures the survey area covers the influence of the crossing structure and captures enough channel information such as slope and bed roughness. In addition, the survey area should be no less than 100 meters as NES-PF requires designers to report the bed invert gradient 50 meters upstream and downstream to determine whether a resource consent is needed.

Equipment and flight plan software are predetermined conditions depending on the accessibility to them. Ground Sample Distance (GSD) can be inferred from the required accuracy. The desired AGL (Above Ground Level) is further deduced from the GSD and camera parameters. This is an empirical method rather than a rigorous calculation. According to Abdullah (2019), for a survey requiring 61 mm of vertical accuracy, AGL should be set to 45 – 60 meters. Other mission parameters such as flight speed, camera angle, and image overlap can also be determined by referring to other flight missions that achieved similar levels of accuracy.

Ground control points (GCPs) are clearly visible marks on the ground with their coordinates measured by survey-grade GPS. The SfM data processing software can use the GCPs as benchmarks to improve the output accuracy. With the help of properly set GCPs the output accuracy can be improved by 5 – 10 times when compared to models that only refer to general on-board GPS unit of the UAV (Turner et al., 2012). But GCPs have an obvious drawback, which is their coordinates need to be measured by survey grade instruments. This will significantly increase the cost and reduce the availability. In this research, the necessity of GCPs will be evaluated.

### **2.3.2 Data collection**

There are two parts to data collection. One is to collect the imagery data for SfM photogrammetry processing. The desirable weather is slightly overcast as there is less glare caused by the reflection of sunlight off the water surface. Wind speed should be checked before the mission to ensure security of flight. The other part is to collect the data for validation. Validation data will be collected by a total station or a differential GPS unit. The validation points need to be evenly spread over the survey area.

### **2.3.3 SfM data processing**

Before processing the data, blurry, duplicate and over-exposed images need to be removed as these images will reduce the quality of the output. The accepted images will then go through SfM software processing. The software used for data processing of this project is Pix4D. It is a cloud-based software that processes all the images in its server. It generates multiple outputs such as orthomosaic, Digital Elevation Model (DEM), point cloud in LAS format and a Geotiff Triangular Irregular Network (TIN) model. The data used for further processing is the orthomosaic and DEM.

### 2.3.4 Water surface model

To apply the refraction correction, the depth of water needs to be extracted from the DEM. The uncorrected elevation data on the DEM of the submerged area is the apparent depth of stream bed. If the water surface elevation can be measured, then the apparent water depth can be derived from subtracting apparent stream bed elevation by water surface elevation. The accurate estimation of water surface elevation is very important as the error in water surface elevation will be directly transferred to the corrected stream bed elevation. One simple approach is to visually identify the edge of water and extrapolate a TIN surface from the identified edge points, where the TIN surface connects the nearest points together. A more complex approach to identify the edge will be covered in section 2.4.

### 2.3.5 Refraction correction

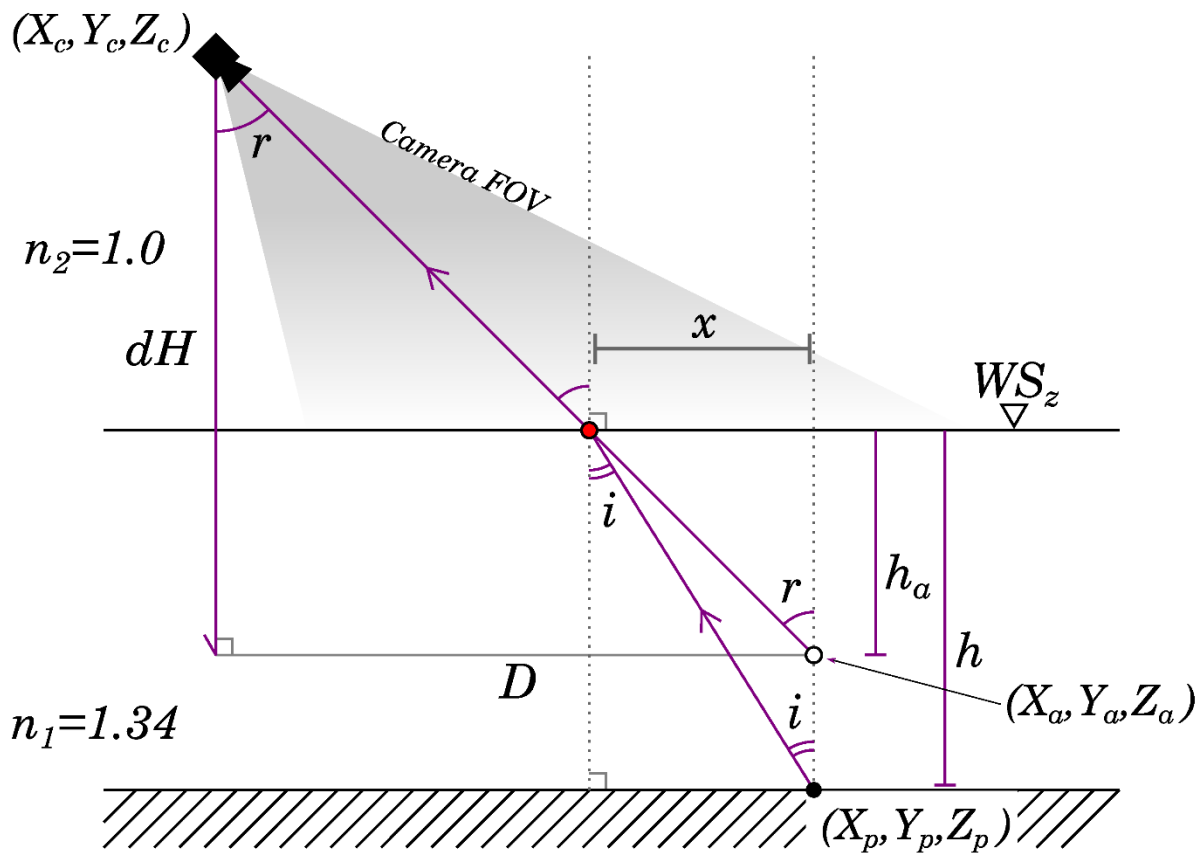


Figure 5. Refraction correction.

Note. From “Bathymetric Structure-from-Motion: extracting shallow stream bathymetry from multi-view stereo photogrammetry,” by J.T. Dietrich, 2017, *Earth Surf. Process. Landf*, 42, 355–364, (<https://doi.org/10.1002/esp.4060>). Copyright 2016 by John Wileys & Sons, Ltd.

Refraction of light as it passes into/out of water is one factor that causes systematic error for elevation of the stream bed. The effect can be explained by Snell’s law. The law states that when

the light passing through two different media such as air and water, the angle of incidence will differ from the angle of refraction. This causes the stream bed appear to be shallower than its real depth. The equation of Snell's law can be expressed as:

$$n_1 \sin \theta_i = n_2 \sin \theta_r$$

where  $n_1$  is the refraction index of water,  $n_2$  is the refraction index of air,  $\theta_r$  is the angle of refraction and  $\theta_i$  is the angle of incidence.

By applying correction factors to apparent depth, we can convert the apparent depth to real depth. The correction factor can be a fixed constant, or it can vary depending on the position.

### **2.3.6 Result validation**

As discussed in Section 2.2, the accuracy of output will be expressed as RMSEs and 95% confidence level in horizontal and vertical direction. A histogram of errors will be drawn to show the distribution of error. An error map will also be generated to show the spatial distribution of the error.

## ***2.4 Improve accuracy***

There is a large amount of literature on UAV photogrammetry-based bathymetry. Many of the studies used innovative approaches in addition to the basic refraction correction to improve accuracy. These techniques have been used in different phases of the data processing process. The techniques that act on different stages can be used together, while for those techniques that act on the same stage, they cannot be used at the same time. The following is a list of techniques that can be used in this project:

### **2.4.1 SOR filter**

SOR filter is a Statistical Outlier Removal tool offered in Cloud Compare. Cloud Compare is an open-source 3D point cloud processing software. It eliminates the noise points in the dense point clouds based on a simple statistical approach to output a cleaner point cloud. A recent study (Emanuele et al., 2020) shows that it is helpful for improving the accuracy of SfM bathymetry outputs. This technique is used before the refraction correction process.

### **2.4.2 Multi-angle refraction correction**

This technique is an advanced refraction correction approach proposed by Dietrich (2017) as an improvement to the previous small angle approximation approach. Instead of assuming all the angles are very small, it corrects the refraction based on each image's camera angle and position. A python script (pyBathySfM) is provided by Dietrich to facilitate the process. And a direct comparison has been made between the multi-angle method and simple angle approximation method. The study shows it effectively reduces the elevation error (Woodget et al., 2019) when the camera is in off-nadir angle. This technique is used in the refraction correction phase. It is a

sophisticated approach. The requirement of data processing skills for this approach is significantly higher than the small angle approach.

### 2.4.3 RGB colour ratio to automatically detect edge of water

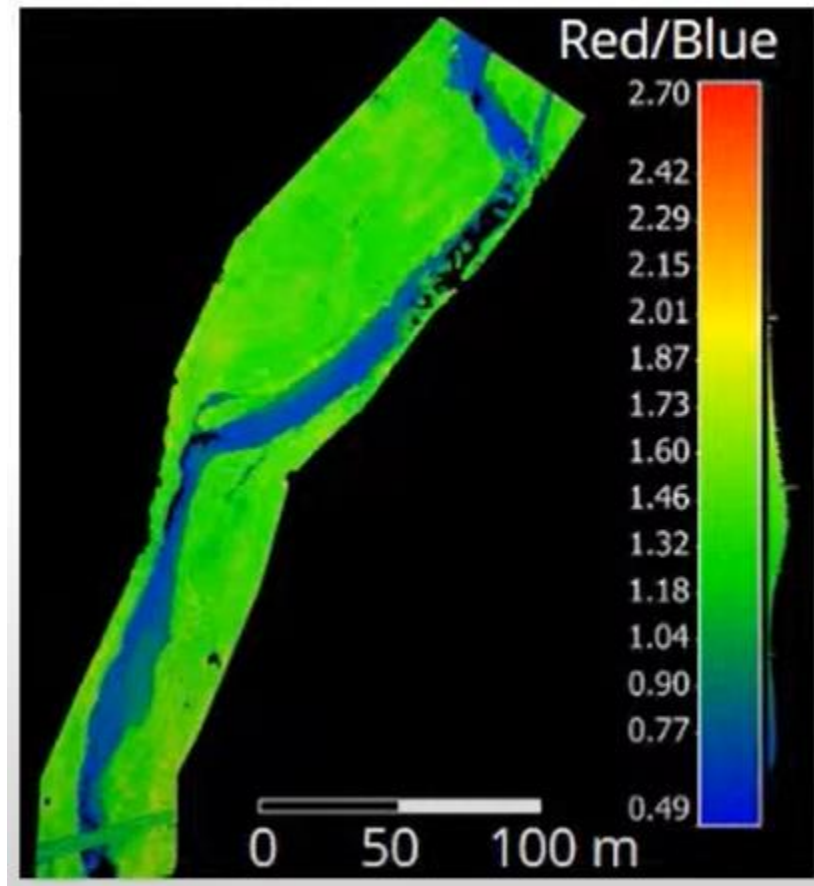


Figure 6. RGB ratio for water edge identification

This technique uses the ratio between red and blue colour bands to detect the edge of water. It helps to reduce the human factor error when classify the edge manually. And it allows identify the edge of water of large area in a timely manner. This technique is used in the stage of generating water surface elevation. It is a less complex technique.

## 2.4.4 Improve visibility of stream bed when water surface is more turbulent



Figure 7. A frame stacking approach to remove surface turbulence

To use this technique, short video is captured instead of still image. Each frame is extracted from the video. All the frames are then converted to the first frame's stage according to the movement of camera and UAV. This helps to detect and remove the unwanted surface turbulence. A study by Partama et al. (2018) first proposed this technique and proved that it is useful to deal with moderate turbulence. This is a sophisticated technique, which is used at the data collection and SfM processing stage.

## 3. Materials and Methods

### 3.1 Study area description

UAV imagery and ground-truthing data were collected from a natural river in the suburb of Halswell (43°35'15.3" S, 172°33'19.3" E), located Southwest of Christchurch, New Zealand. A 50 m long section of stream with a depth of 0 to 0.9 m was selected as the study area. The stream bed consisted mainly of medium-sized silty gravels. The survey was carried out on an overcast

day with little wind. Flow velocities were low so that only a small amount of surface waves were present. Both photogrammetry and GNSS data were collected on 17<sup>th</sup> July 2021.

### ***3.2 Ground control points set-up and validation data collection***

The UAV-SfM technique requires georeferenced images. The georeferencing can be performed with the UAV's inbuilt GNSS receiver or with the assistance of ground control points (GCPs). GCPs are markers that are clearly visible from the sky with the coordinates measured by survey-grade GNSS receivers. Since part of the case study is to test if it is necessary to use GCPs to achieve the level of accuracy required, four GCPs were established, one on each corner of the study area. The coordinates of the GCPs were measured with a Trimble GeoX7 GNSS coupled with a Zephyr2 rover. The positioning data was post processed in Trimble Pathfinder Office to achieve a reported accuracy of 5 to 10 cm. The validation data was collected with the same approach. 121 validation points were randomly distributed and measured across the submerged area. All the GNSS data was collected in WGS84 then converted to NZTM2000 projections. The locations of the GCPs and validation points are shown in Figure 8.



Figure 8. GCPs and validation points of the first study area.

### ***3.3 Photogrammetry data acquisition***

The aerial imagery was captured using a DJI Mavic 2 Pro drone with the factory camera. The camera has a 13.2 mm x 8.8 mm CMOS sensor with a focal length of 10.3 mm. Two sets of images were captured at 30 m and 50 m AGL (above ground level). When images are captured from 30

m and 50 m above ground level, the ground sample distance of the image is 0.7 cm and 1.2 cm respectively. The flight is automated along a double-grid path over the area of interest using Pix4D Capture with a 90% front/side overlap and 10 degrees off-nadir camera angle. The speed of flight is set to 2 m/s to avoid capturing blurred image. For the 30 m mission, 48 images were captured, and 3 images were removed due to redundancy. For the 50 m mission, 25 images were captured and used for processing.

### ***3.4 Structure from Motion processing***

The two sets of images were imported in Agisoft Metashape Pro version 1.5.2.7838, which is a commercial SfM processing software that integrates all the photogrammetry routines such as image stitching, camera alignment, geometry building, georeferencing, error reporting etc. Three SfM projects were performed separately, which are: (i) images taken at 30 m AGL without using GCPs, (ii) images taken at 50 m AGL with GCPs and (iii) images taken at 30 m AGL with GCPs. For the latter two projects, GCPs were imported to Agisoft Metashape Pro to recalibrate the camera positions and to correct the construction of the point cloud. For each project, the LAS point cloud, DEM and LRGB orthomosaic were exported for later use. In the point clouds, some noise points presented under the culvert. These noise points will be removed in the next steps to ensure the overall quality of the models.

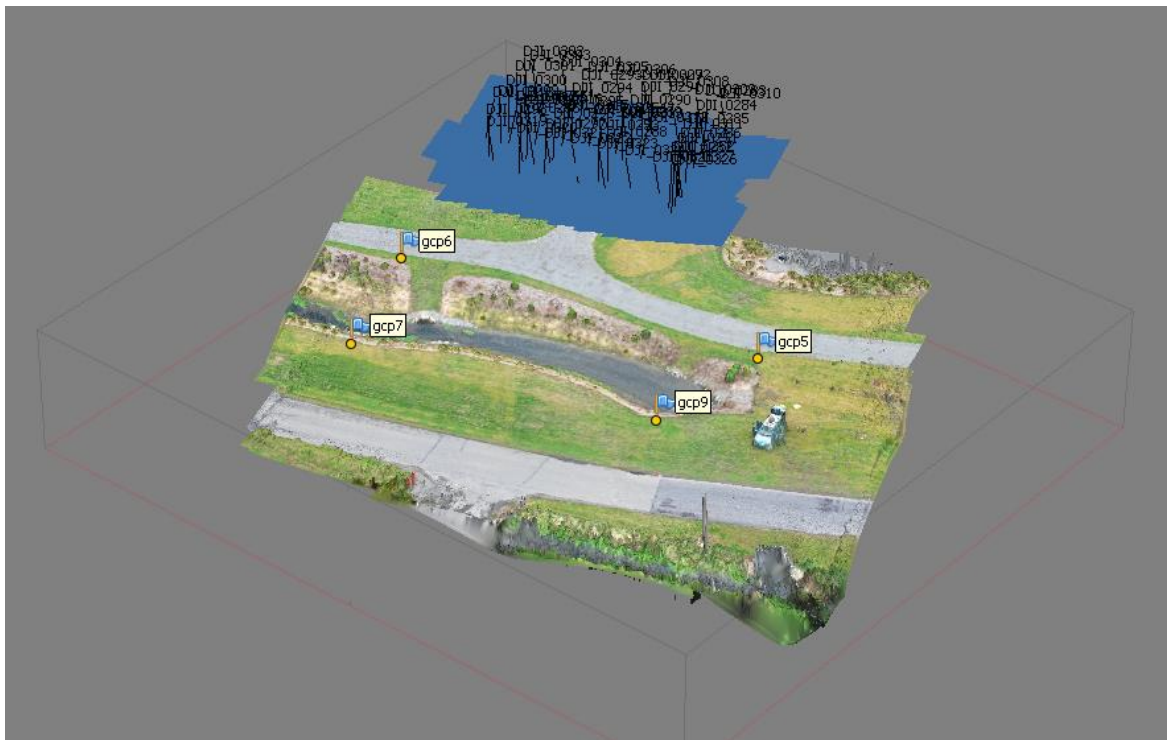


Figure 9. SfM model generated by Agisoft Metashape Pro

### ***3.5 Refraction correction***

As discussed in Section 2.3.5, the refraction of light at the water-air interface caused the point cloud of the submerged area to have an underestimated elevation. Refraction correction should therefore be applied to correct the underestimated elevation. The refraction correction process consists of three steps; the first step is to determine the water surface elevation, the second is to extract the apparent water depth and the third is to calculate the corrected water depth and regenerate the underwater portion of the point cloud based on the corrected water depth. For each of the 3D models generated in the previous section, refraction corrections were made using three different methods, the first being a small-angle correction method, the second being a multi-angle correction method and the third without correction as a control dataset.

#### **3.5.1 Water surface model**

The water surface model is essential for both methods of refraction correction. As the water surface was relatively still during the UAV images collection, the water surface is assumed to be planar. To construct the water surface model, the edge of water needs to be identified. In ArcGIS, a red / blue colour ratio layer is used to help identify the edge of water. The water edge was then manually reviewed and edited to make sure it is error-free. A shapefile feature is exported to CloudCompare. A mesh representing the water surface is fitted to the shapefile, i.e. the water surface model.

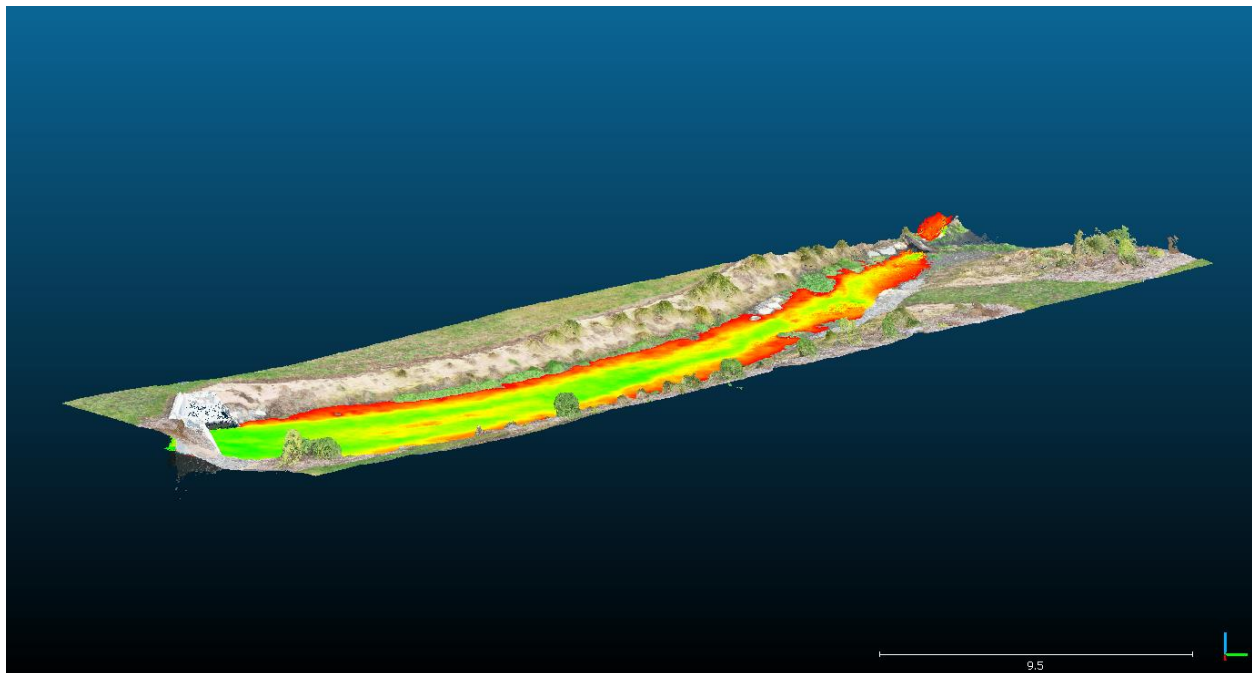


Figure 10. Water surface model constructed in Cloud Compare

### 3.5.2 Small angle correction processing

A small angle approximation approach (Woodget et al., 2015) allows the calculation of real depth  $h$  from apparent depth  $h_a$  without knowing the incidence or refraction angles. As the image is captured in a small-angle off-nadir direction, if it is assumed that the angles are very small,  $\sin\theta$  would be very close to  $\tan\theta$ . Actual depth  $h$  can be derived from simple calculation as follows:

$$x = h_a \times \tan\theta_r = h \times \tan\theta_i$$

$$\tan\theta_r = 1.34\tan\theta_i$$

$$h = 1.34h_a$$

This allows a single correction factor to be applied throughout the entire submerged area. The small-angle approach is a simple and fast method for refraction correction. First the DEM generated by SfM is imported into ArcGIS. By using the raster calculator, the apparent depth of water is calculated by subtracting uncorrected stream bed elevation from the water surface model. The apparent depth is then multiplied by a constant of 1.34, which is the ratio of the refraction index of water to that of air. The corrected water depth is then subtracted from the water surface model's elevation to get the corrected stream bed elevation. Figure 11 shows the corrected elevation of the submerged area ranges from 21.68 m to 23.24 m.



Figure 11. The DEM of the submerged area by small-angle method

### 3.5.3 Multi-angle correction processing

Instead of applying a constant correction factor to the whole submerged area, the multi-angle method repeatedly corrects the elevation of each point in the submerged part of the point cloud with the accompanying camera position and direction. This iterative approach and accompanying Python software pyBathySfM v4.5 are proposed by Dietrich (2017). To use the software, the prepared point cloud with apparent depth of water and water surface elevation, the focal length and sensor size of the camera, the camera position and direction (x, y, z coordinates, yaw, pitch, and roll) of each image are required. The preparation of the point cloud is done in CloudCompare version 2.12 alpha. First, the elevation of the submerged area is subtracted from the water surface model to obtain the apparent water depth. The apparent water depth is then added back to uncorrected elevation to assign the water surface elevation to each point. The camera position and direction are exported from the SfM software; Agisoft Metashape Pro. The focal length and sensor size are found online. The three prepared files are then imported into pyBathySfM. PyBathySfM will generate a new point cloud with the corrected elevation. Figure 12 shows the cross-sectional profile of stream bed before and after using multi-angle correction. The process from 3.5.1 to 3.5.3 is repeated for the three SfM models (30 m, 50 m, 30 m without GCPs).

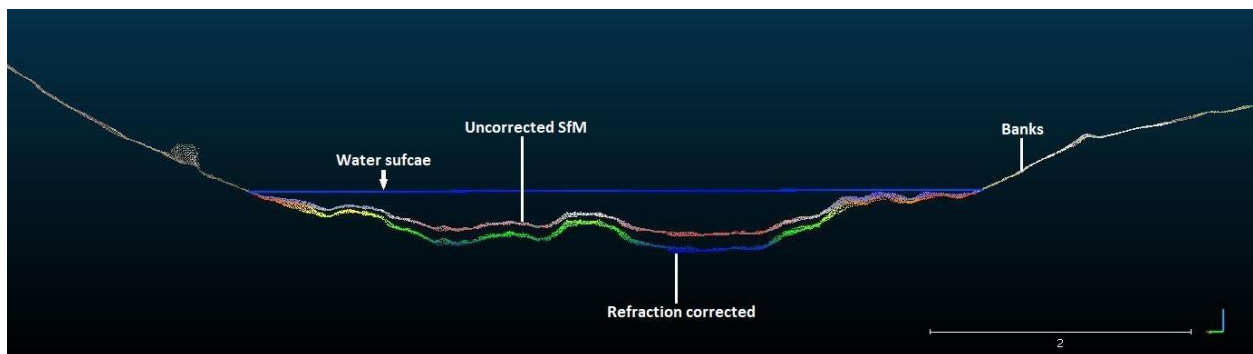


Figure 12. Cross-sectional profile of stream bed before and after using multi-angle correction.

### 3.6 Validation of data

The validation survey points are used to check the accuracy and precision of all the models. First, the corrected point cloud of each model is rasterised using the 'LAS to Raster' tool in ArcGIS. Despite the high density of the point cloud data, there are still gaps between the points. Therefore, when generating the raster, these gaps need to be filled by interpolation from nearby points. The difference caused by the different interpolation methods is almost negligible. Next, the 'Extract Multi Values to Points' tool is used to extract elevation value from all the raster layers to the validation survey points. The point feature with different elevation data is then exported to Excel for statistical analyses. Also, the corrected point cloud is exported to CloudCompare to generate cross-sectional profiles of the corrected results.

### ***3.7 Test the proposed workflow in another site***

To test the consistency of the workflow in various stream conditions, a secondary study was performed. The second study area is located Southeast of Christchurch at 43°35'52" S, 172°32'37.3" E. The stream has a deeper bed and the flow rate was slightly higher compared to the stream in first study. There are 10 control points used for the secondary study. To test the accuracy, 24 validation points were collected along three cross-sectional direction as shown in Figure 13. There are 68 images collected with the same DJI UAV at 30 m AGL. The workflow used to process the data was that with the best accuracy found during the first study, which used GCPs to build SfM model and corrected for refraction with the multi-angle method.



Figure 13. GCPs and the validation points of the second study area.

## 4. Results

### 4.1 SfM quality

There are three SfM models generated, which are the model generated from images taken 30 m above ground level, the model from the same images but without using GCPs, and the model from images taken 50 m above ground level. Some SfM model quality indicators are shown in Table 2. These indicators are obtained from the processing report generated by Agisoft Metashape Pro. The reprojection error indicates the overall quality of the models are good. However, the reprojection error of models built with GCPs are higher than the error of model without GCPs. It suggests that using these GCPs may introduce slight distortions to the model. The distortion may be caused by the GNSS equipment's limited accuracy comparing to the accuracy of the SfM model itself.

Table 2. Quality indicators of the SfM models

Model	Images used	Ground sample distance	Point density	Reprojection error	Processing time
30m	52	1.35 cm/pixel	5500 points/m <sup>3</sup>	1.37 pixel	40 min
30m nogcp	52	1.35 cm/pixel	5520 points/m <sup>3</sup>	1.08 pixel	40 min
50m	25	2.27 cm/pixel	1940 points/m <sup>3</sup>	1.27 pixel	10 min

### 4.2 Error statistics

Three SfM models combined with two correction methods and data from exposed area result in 9 different groups of measurements. To assess the accuracy of each group of data, the error is derived from the difference between the survey point's water depth and water depth extracted from the DEMs. Table 2 shows the mean, standard deviation, RMSE, the minimum and the maximum value of the errors of each group of data, where SfM\_30 = uncorrected SfM model from image taken 30 m above ground level, sa\_50 = small angle correction with SfM model from image taken 50 m above ground level, ma = multi-angle correction, SfM30\_ng means model built from the images captured 30 m above ground without using GCPs, these abbreviations also apply to the other tables and figures.

Table 3. Error statistics by group, all values have units in meters

model	SfM_30	sa_30	ma_30
mean	-0.092	-0.020	-0.011
std	0.148	0.141	0.140
RMSE	0.177	0.144	0.145
min error	-0.468	-0.350	-0.338
max error	0.233	0.295	0.312
model	SfM_50	sa_50	ma_50

<b>mean</b>	-0.096	-0.025	-0.022
<b>std</b>	0.151	0.150	0.151
<b>RMSE</b>	0.181	0.154	0.155
<b>min error</b>	-0.447	-0.322	-0.316
<b>max error</b>	0.242	0.306	0.313

<b>model</b>	<b>SfM30_ng</b>	<b>sa30_ng</b>	<b>ma30_ng</b>
<b>mean</b>	-0.121	-0.035	-0.026
<b>std</b>	0.196	0.141	0.145
<b>RMSE</b>	0.233	0.147	0.149
<b>min error</b>	-1.355	-0.307	-0.305
<b>max error</b>	0.254	0.329	0.349

The ma\_30 model has the smallest mean of -0.011 m and standard deviation of 0.14 m. The sa\_30 model and sa30\_ng model has the smallest RMSE of 0.144 m. Figure 14 shows the distribution of error of each model. The models built from images captured 30 m above ground level with the use of GCPs have mean values closer to zero.

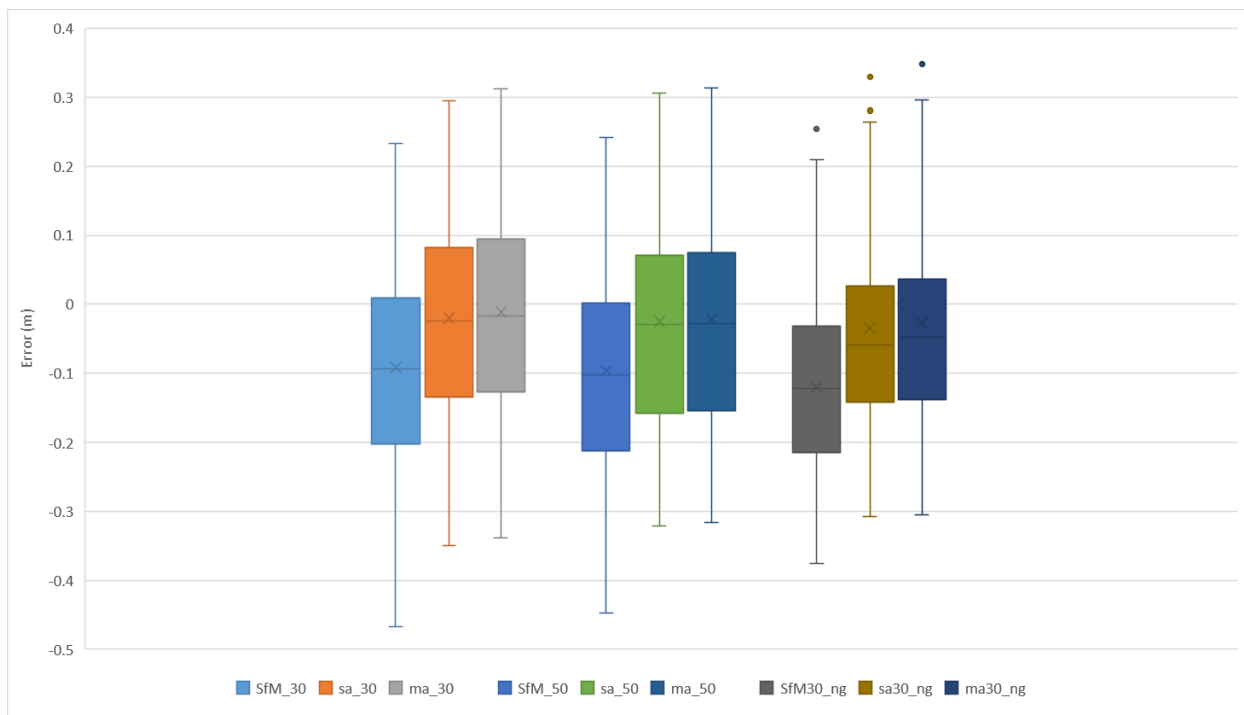


Figure 14. Distribution of errors by group

### ***4.3 Ground control points***

The use of GCPs greatly reduced the mean error. The mean error is reduced by 24% for uncorrected models, 43% for small angle correction models, and 58% for multi-angle models. However, for models corrected by small-angle or multi-angle method, the use of GCPs did not significantly reduce the standard deviation and the RMSE. The standard deviation is reduced by 0% and 4% while the RMSE is reduced by 3% and 5%, which are only about 0 to 7 mm. Setting up GCPs requires a relatively small amount of time if accessibility is not a concern. However, it requires the use of a more accurate GNSS instrument to measure the coordinates of the GCPs. Due to the limited accuracy of the GNSS instruments used in this experiment, the models with the use of GCPs are distorted as the interquartile range (IQR) of models with GCPs are larger than the models without GCPs, which is consistent with the reprojection error shows in Table 2.

### ***4.4 Flight height***

The model built from 30 m images achieved a better accuracy than the model built from 50 m images. The mean error reduced by 4 mm for uncorrected model, 5 mm for small-angle correction model and 12mm for multi-angle correction model. The standard deviation reduced by 3 mm, 9 mm, 11 mm and the RMSE reduced by 4 mm, 11 mm, 13 mm for uncorrected, small-angle, and multi-angle models respectively.

The advantage of capturing images from an altitude of 50 metres is that a larger area can be covered in a shorter flight time. However, for smaller projects such as stream survey, even from lower altitudes, the total flight time will not exceed 30 minutes. However, the flight altitude should not be too low, as low altitudes tend to blur the image and the ground sample distance of 0.7 cm per pixel at 30 m above ground level is small enough. A smaller ground sample distance will not further improve the accuracy of the model. Therefore, the recommended flight height for culvert design stream survey is 30 metres. For safety concerns, the flight height should be 1.5 times higher than the height of the highest object at the surveying site and lower than the minimum flight height required by law.

Figure 15 shows the magnitude of error at different water depth of different models. In the uncorrected models, the error shows a moderate level (ca. 0.4  $R^2$ ) of correlation to the depth of water, which suggesting that refraction between water and air introduces systematic errors into the SfM models. After applying the small-angle corrections, the correlation between error and water depth is significantly reduced. The very small R-Squared values indicate the correlations between error and depth of water are no longer significant. The  $R^2$  value for the sa30\_ng model is only 0.00024, while the  $R^2$  values for the other two models are slightly higher, but still significantly lower than the uncorrected model. In addition, the slope of the regression line also reduced after applying the small-angle corrections, reaching around 0.005.

## 4.5 Error versus water depth

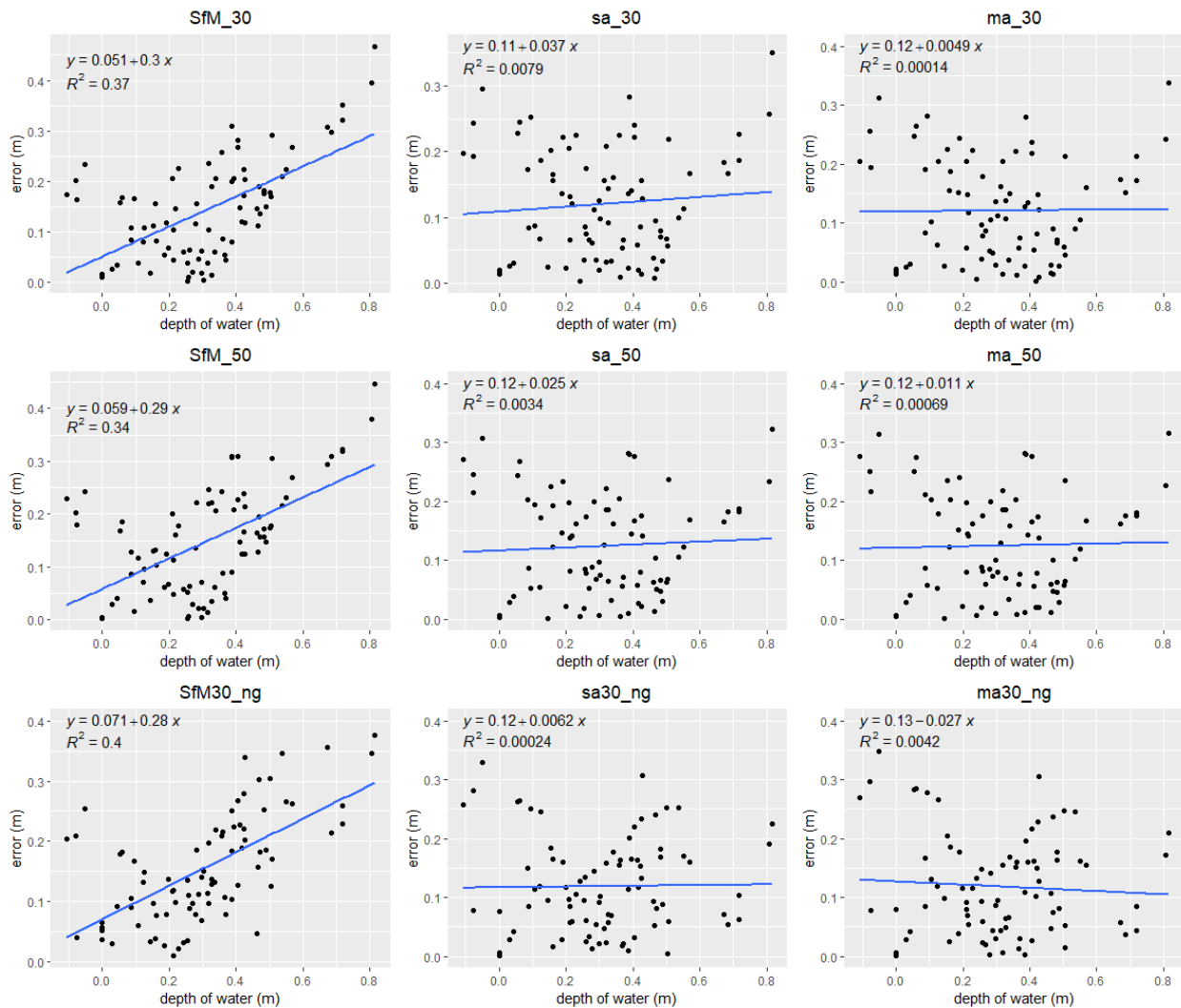


Figure 15. relative error versus depth of water by group

When applying the multi-angle corrections to the SfM models, the correlation between error and water depth is further reduced to a lower level except the ma30\_ng model. The reason for the negative correlation of ma30\_ng model is unknown, but the  $R^2$  value of 0.0042 indicates that the correlation is not significant. The slope of the regression line was maintained at the same level as the small-angle correction models.

## 4.6 Performance of refraction correction

The performance of each model for estimating water depth is shown in Figure 16. As expected, the performance of the three uncorrected models is poorer than the corrected models. The model from images captured 30 m above ground level with multi-angle correction achieved a gradient closest to one. But its goodness-of-fit is slightly poorer than the same model with small-

angle correction. For the models built from 50 m image data, the difference between the performance of small-angle and multi-angle correction is even smaller. This is probably because when the camera is shooting from 50 meters height, the incidence angle of refraction is smaller, which is more in line with assumption of small-angle correction. Thus, there is no significant improvement of the multi-angle correction. In addition, the gradient and goodness-of-fit of the three models built from 30 m data are all better than the 50 m models, which suggests 30 m is a better height for image acquisition.

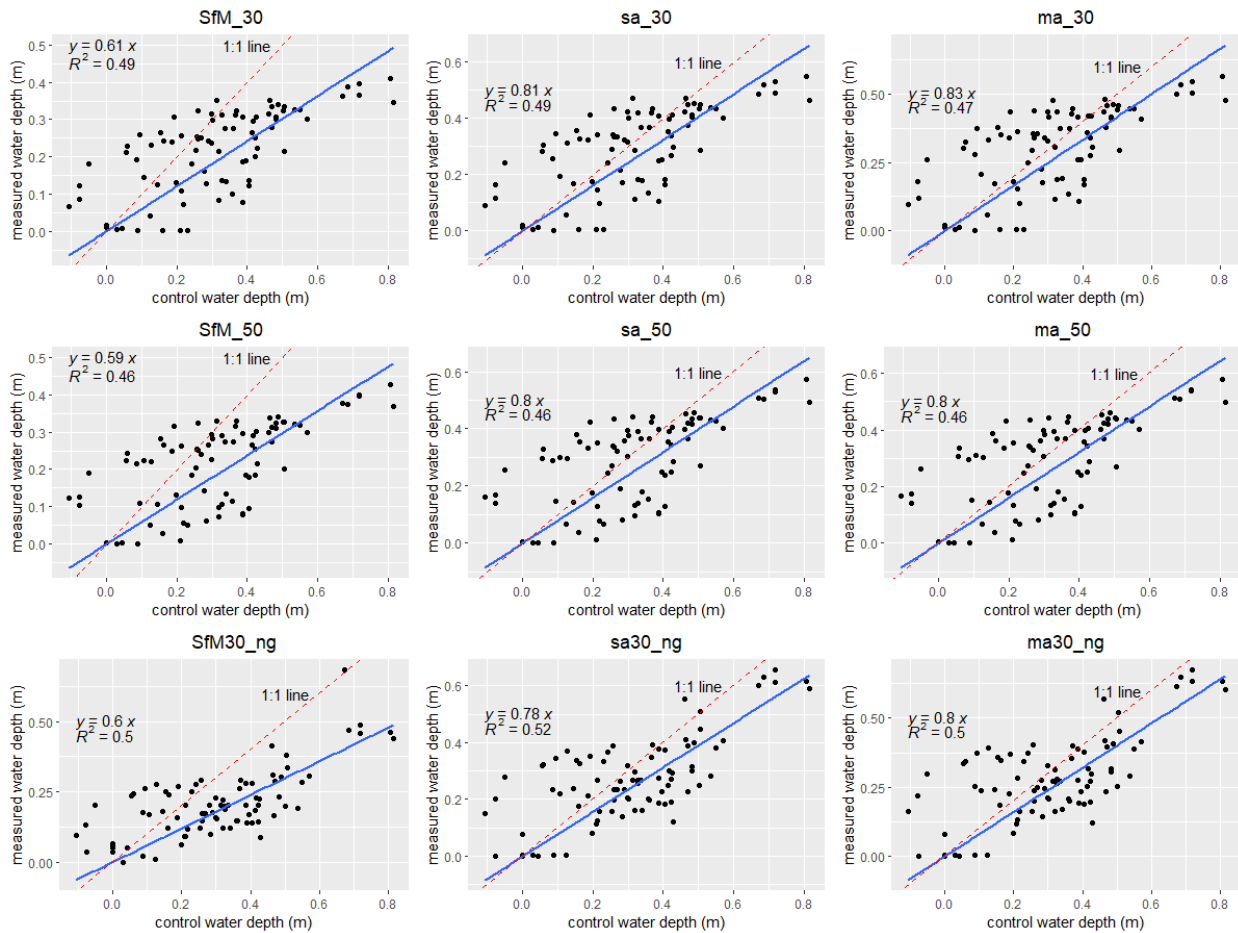


Figure 16. scatter plot of measured water depth versus control data of water depth.

### 4.7 Results from the second study

As shown in Figure 17, the streambed after correcting for refraction is closer to the validation points than the uncorrected model. 24 validation points along three cross-sections were used to check the accuracy. The error is calculated for the uncorrected SfM model and the model corrected by multi-angle method. For the uncorrected model, the mean error is 0.241 m, the standard deviation is 0.261 m, the RMSE is 0.352 m. For the corrected model, the mean of error is 0.022 m, the standard deviation is 0.105 m and the RMSE is 0.105 m. It showed that the proposed workflow can achieve consistent accuracy in different streams.

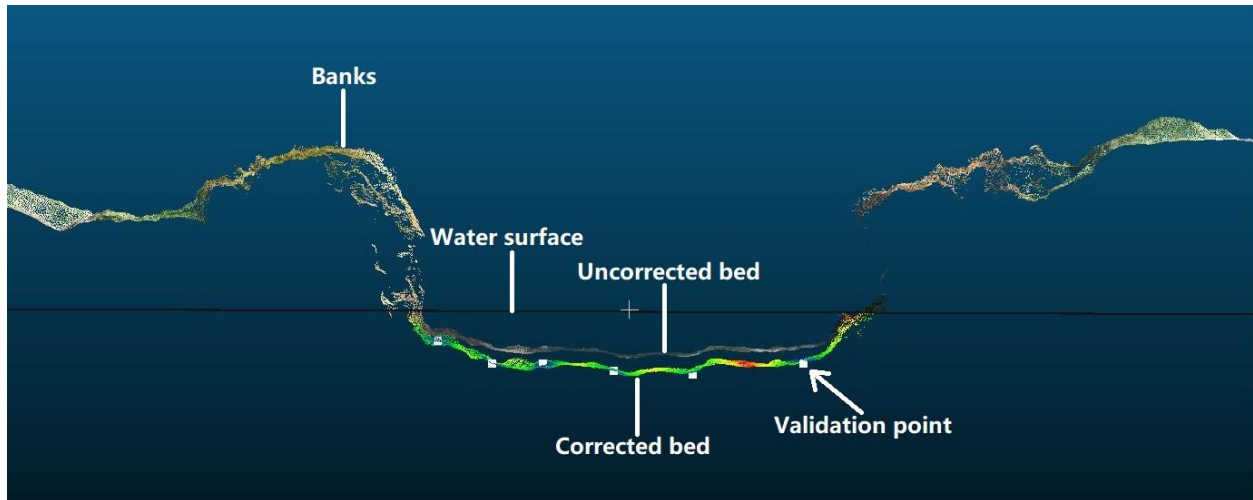


Figure 17. Cross-sectional profile of stream bed from the second study area

## 5. Discussion

### 5.1 *Relative accuracy versus absolute accuracy*

Relative accuracy is the accuracy of the dimensions of an object in a model comparing to its real-world dimensions. For example, if the distance from point A to point B is measured in the model as 5 metres, and this is the same as the distance from point A to point B in real-world, the model has relative accuracy.

Absolute accuracy is the accuracy of the position of an object in the model comparing to its position in the real-world. If points A and B are far away from their positions in the real world, then the absolute accuracy is low, even if the relative accuracy is high.

In culvert design, the important parameters such as depth, shape and slope of the stream bed require relative accuracy. It is less important to achieve a high absolute accuracy since it is unnecessary to know the coordinates. Even if overlaying the model to other maps is required, it is possible to manually overlay the model to other maps then assign offset values to the existing coordinates.

The absolute accuracy is derived from the difference between the survey point's elevation and the elevation extracted from the DEMs. Table 3 shows the absolute error of elevation by group. As expected, the 30 m model without using GCPs had the worst absolute accuracy, which the mean errors and RMSE greater than 8 m. The standard deviation is consistent with the relative accuracy as it describes the dispersion of the dataset itself. The other models that used GCPs had

a smaller difference between their absolute and relative accuracy, as GCP has helped the models to correct for the coordinate errors.

Table 4. Absolute error of elevation by group, all values have units in meters

model	SfM_30	sa_30	ma_30
mean	0.188	0.115	0.107
std	0.150	0.147	0.150
RMSE	0.243	0.189	0.186
min error	-0.135	-0.197	-0.214
max error	0.566	0.448	0.436

model	SfM_50	sa_50	ma_50
mean	0.212	0.141	0.137
std	0.153	0.151	0.152
RMSE	0.264	0.209	0.207
min error	-0.124	-0.189	-0.195
max error	0.565	0.440	0.434

model	SfM30_ng	sa30_ng	ma30_ng
mean	-8.823	-8.909	-8.918
Std	0.197	0.142	0.146
RMSE	8.822	8.908	8.917
min error	-9.196	-9.272	-9.291
max error	-7.587	-8.635	-8.637

## 5.2 Efficacy of the different workflows

The combination of several data acquisition and correction methods covered in this paper result in different lengths of the total projects and require different equipment and software as well as skills to use these equipment and software. For data acquisition, the main differences being the flight altitude and whether GCPs are used. As shown in Table 2, the RMSE for the model without GCP was only 3 to 4 mm larger than that of the model with GCP. Also, the RMSE is even smaller than the models built from 50 m image. Therefore, it is important to acquire the image at lower altitude, where the situation allows. GCPs should be deployed where more accurate GNSS equipment is available, and time allows. According to the results for this experiment, GCPs can also be left out when there is no access to accurate GNSS equipment.

Setting up GCPs for a large area could add significant time to the workflow, a better solution is using an RTK UAV. RTK UAVs are drones with on-board RTK units that improve the accuracy of positioning. By performing RTK processing with an active base station, the drone can record

accurate positioning information when taking images, thus saving time in setting up the GCPs and achieving the same accurate results as using the GCPs.

Next is the refraction correction. As shown in Figure 9, both correction methods can significantly reduce the mean and RMSE of error. Therefore, it is necessary to perform refraction correction for the SfM model. The workflow and results of the two correction methods need to be compared.

The small-angle correction method involves two software for the entire process. The uncorrected DEM generated by SfM software is imported into ArcGIS. The computed water depth is multiplied by a fixed refraction index of 1.34. The result is the corrected water depth. In contrast, the process of multi-angle correction is more complex and involves more software. First, the SfM software is used to generate uncorrected point cloud and camera angles. The uncorrected point cloud is then edited by CloudCompare to prepare the data ready for correction. The point cloud, together with the camera angles and sensor dimensions, is inputted to pyBathySfM for the final correction. The correction process can take anywhere from a few minutes to approximately two hours depending on the size of the area of interest. The workflow is more complex than small-angle correction, but the learning curve is relatively smooth. It can take hours-to-days for a person with intermediate computer skills to learn.

It is worth noting that due to the small area of the site, the topography is relatively simple, no canopy cover is present, no sudden change of elevation and the water surface relatively still, the difference between the results of the small-angle correction and the multi-angle correction is small. The multi-angle correction still achieved a slightly higher accuracy, but the improvement was limited due to these factors. In research carried out on a 600-m-long reach (Woodget et al., 2019), where the topographic and water surface condition are more complex, the RMSE of water depth was improved by ca. 0.05 m, which is an significant improvement. Table 5 summarise the different methods used in this study in terms of performance and efficacy.

Table 5. comparison of different accuracy improvement methods

Method	using GCPs	Small-angle correction	Multi-angle correction
Time	10 min – ~2 hours, depends on site and devices used	Several minutes	Can take one to a few hours depending on size of survey site
Pros	Significantly improves the mean relative accuracy and georeferencing accuracy	Simple and fast workflow regardless of the survey area, removes systematic error caused by refraction effectively	Removes most systematic error caused by refraction
Cons	Requires accurate GNSS devices or total station measuring from a known coordinate; time consuming	Less accurate than multi-angle method when the site has complex water surface and terrain, or when larger off-nadir angle of camera is used (Puig-Mengual et al., 2021)	Learning curve is a bit steep since multiple software involved; processing time increases quickly with site area; limited improvement of accuracy at sites with simple topography

Comments	Ensures the quality of SfM models, especially for larger sites; highly recommended with access to high accuracy GNSS devices; can be replaced by RTK-UAV	It is important to use a low off-nadir angle of the camera; in this site the small-angle method is outperformed the multi-angle method due to the simplicity of the site	Theoretically this method would outperform the small-angle method. This method has the great potential to be automated and integrated to advanced SfM software
----------	--	--	--

## 6. Conclusion

To understand if UAV-SfM survey can meet the level of accuracy required by forestry stream crossing design purpose, the assessments of accuracy of several different workflows for UAV-SfM topographic stream survey have been performed. The models without refraction correction shows significant systematic errors caused by refraction of light in water, which leads to an underestimation of water depth and thus inaccurate stream bed topography. Both refraction correction methods (small-angle and multi-angle) can remove the systematic errors from the models successfully. In the relatively simple site surveyed in the first study, the multi-angle correction achieved a lower mean error than the small-angle correction, but the precision, i.e. the error distribution has not been improved. The using of GCPs helps improve the mean errors by about 50%. It additionally ensures the georeferencing of the model. However, in terms of relative accuracy, for the models with refraction correction, the improvement in precision by using GCPs is almost negligible. This implies for small sites with simple topography, steady water surface and no canopy cover, the use of GCPs is not critical to achieve an acceptable relative accuracy. Nevertheless, the use of refraction correction is necessary. In addition, flight height of image acquisition has an impact on the accuracy of the models. A 30 m above-ground-level flight height is a good guide for this kind of survey. The accuracy of the second study's results is very close to the first study, which shows the proposed workflow can achieve consistent accuracy under different stream conditions. The UAV-SfM survey with refraction correction technique has the potential to achieve promising survey results for forestry stream crossing design in an efficient manner.

## 7. References

- Abdullah, Q. (2019). Geospatial Data Quality and Accuracy: The State-of-the-Practice Agency, W. K. N. T. (2021, 31 March 2021). State highway professional services contract proforma manual. In. Retrieved 15 May 2021, from
- Akgul, M., Yurtseven, H., Gulci, S., & Akay, A. E. (2018). Evaluation of UAV- and GNSS-Based DEMs for Earthwork Volume. *Arabian Journal for Science and Engineering*, 43(4), 1893-1909. <https://doi.org/10.1007/s13369-017-2811-9>
- ASPRS. (2014). ASPRS Accuracy Standards for Digital Geospatial Data. American Society of Photogrammetry and Remote Sensing,
- Brown, K., & Visser, R. (2018). Adoption of emergent technology for forest road management in New Zealand. *NZ J For*, 63(3), 23-29.
- De Gouw, S., Morgenroth, J., & Xu, C. (2020). An updated survey on the use of geospatial technologies in New Zealand's plantation forestry sector. *New Zealand Journal of Forestry Science*, 50.
- Dietrich, J. T. (2017). Bathymetric Structure - from - Motion: extracting shallow stream bathymetry from multi - view stereo photogrammetry. *Earth Surface Processes and Landforms*, 42(2), 355-364. <https://doi.org/10.1002/esp.4060>
- Emanuele, P., Nives, G., Andrea, C., Carlo, C., Paolo, D., & Andrea Maria, L. (2020). Bathymetric Detection of Fluvial Environments through UASs and Machine Learning Systems. *Remote Sensing*, 12(24), 4148.
- Forest Growers Levy, T., New Zealand Forest Owners, A., & New Zealand Farm Forestry, A. (2020). *New Zealand forest road engineering manual* (Updat February 2020. ed.). NZ Forest Owners Association.
- Franklin, P., Gee, E., Baker, C. F., Bowie, S., & National Institute of Water and Atmospheric, R. (2018). *New Zealand fish passage guidelines: for structures up to 4 metres*. NIWA Taihoro Nukurangi.
- Iglhaut, J., Cabo, C., Puliti, S., Piermattei, L., O'Connor, J., & Rosette, J. (2019, 2019/09/01). Structure from Motion Photogrammetry in Forestry: a Review. *Current Forestry Reports*, 5(3), 155-168. <https://doi.org/10.1007/s40725-019-00094-3>
- Infrastructure, N. S. D. (2002). *Geospatial Positioning Accuracy Standards*.
- LINZ. (2009a). *Standard for the geospatial accuracy framework*. [https://www.linz.govt.nz/system/files\\_force/media/regulatory-documents/25005-Standard%20for%20the%20geospatial%20accuracy%20framework%20-%20LINZS25005\\_4.pdf?download=1](https://www.linz.govt.nz/system/files_force/media/regulatory-documents/25005-Standard%20for%20the%20geospatial%20accuracy%20framework%20-%20LINZS25005_4.pdf?download=1)
- LINZ. (2009b). *Standard for the geospatial accuracy framework*. [https://www.linz.govt.nz/system/files\\_force/media/regulatory-documents/25005-Standard%20for%20the%20geospatial%20accuracy%20framework%20-%20LINZS25005\\_4.pdf?download=1](https://www.linz.govt.nz/system/files_force/media/regulatory-documents/25005-Standard%20for%20the%20geospatial%20accuracy%20framework%20-%20LINZS25005_4.pdf?download=1)
- Partama, I. G. Y., Kanno, A., Ueda, M., Akamatsu, Y., Inui, R., Sekine, M., Yamamoto, K., Imai, T., & Higuchi, T. (2018). Removal of water - surface reflection effects with a temporal minimum filter for UAV - based shallow - water photogrammetry. *Earth Surface Processes and Landforms*, 43(12), 2673-2682.

- Piermattei, L., Karel, W., Wang, D., Wieser, M., Mokroš, M., Surový, P., Koreň, M., Tomašík, J., Pfeifer, N., & Hollaus, M. (2019). Terrestrial structure from motion photogrammetry for deriving forest inventory data. *Remote Sensing*, 11(8), 950.
- Puig-Mengual, C. A., Woodget, A. S., Muñoz-Mas, R., & Martínez-Capel, F. (2021). Spatial validation of submerged fluvial topographic models by mesohabitat units. *International Journal of Remote Sensing*, 42(7), 2391-2416.
- Riedinger, L. (2020). *Structure-from-Motion Photogrammetry as a Tool for Slash Pile Volume Measurement* University of Canterbury]. <https://forestengineering.org/wp-content/uploads/2020/11/2020-SfM-Slash-Pile-Measure-Luke-Riedinger.pdf>
- Rossi, P., Mancini, F., Dubbini, M., Mazzone, F., & Capra, A. (2017). Combining nadir and oblique UAV imagery to reconstruct quarry topography: methodology and feasibility analysis. *European Journal of Remote Sensing*, 50(1), 211-221.
- Transportation, U. S. D. o. (2018). SURVEYING AND MAPPING. In *Project management and design manual* (pp. 5-16). [https://flh.fhwa.dot.gov/resources/design/pddm/Chapter\\_05.pdf](https://flh.fhwa.dot.gov/resources/design/pddm/Chapter_05.pdf)
- Turner, D., Lucieer, A., & Watson, C. (2012). An automated technique for generating georectified mosaics from ultra-high resolution unmanned aerial vehicle (UAV) imagery, based on structure from motion (SfM) point clouds. *Remote Sensing*, 4(5), 1392-1410.
- United States. Forest Service. Stream-Simulation Working Group., & Technology & Development Program (U.S.). (2008). *Stream simulation : an ecological approach to providing passage for aquatic organisms at road-stream crossings*. National Technology and Development Program.
- Woodget, A., Carbonneau, P., Visser, F., & Maddock, I. P. (2015). Quantifying submerged fluvial topography using hyperspatial resolution UAS imagery and structure from motion photogrammetry. *Earth Surface Processes and Landforms*, 40(1), 47-64.
- Woodget, A. S., Dietrich, J. T., & Wilson, R. T. (2019). Quantifying Below-Water Fluvial Geomorphic Change: The Implications of Refraction Correction, Water Surface Elevations, and Spatially Variable Error. *Remote Sensing*, 11(20), 2415.
- Zulkipli, M. A., & Tahar, K. N. (2018). Multirotor UAV-Based Photogrammetric Mapping for Road Design. *International journal of optics*, 2018, 1-7. <https://doi.org/10.1155/2018/1871058>